NASA/TM—2005–213848

A "Kane's Dynamics" Model for the Active Rack Isolation System

Part Three: Addition of Umbilicals to the Nonlinear Model

J.K. Rupert
Dynetics, Inc., Huntsville, Alabama

R.D. Hampton
United States Military Academy, West Point, New York

G.S. Beech
Marshall Space Flight Center, Marshall Space Flight Center, Alabama

February 2005

The NASA STI Program Office…in Profile

Since its founding, NASA has been dedicated to the advancement of aeronautics and space science. The NASA Scientific and Technical Information (STI) Program Office plays a key part in helping NASA maintain this important role.

The NASA STI Program Office is operated by Langley Research Center, the lead center for NASA's scientific and technical information. The NASA STI Program Office provides access to the NASA STI Database, the largest collection of aeronautical and space science STI in the world. The Program Office is also NASA's institutional mechanism for disseminating the results of its research and development activities. These results are published by NASA in the NASA STI Report Series, which includes the following report types:

- TECHNICAL PUBLICATION. Reports of completed research or a major significant phase of research that present the results of NASA programs and include extensive data or theoretical analysis. Includes compilations of significant scientific and technical data and information deemed to be of continuing reference value. NASA's counterpart of peer-reviewed formal professional papers but has less stringent limitations on manuscript length and extent of graphic presentations.

- TECHNICAL MEMORANDUM. Scientific and technical findings that are preliminary or of specialized interest, e.g., quick release reports, working papers, and bibliographies that contain minimal annotation. Does not contain extensive analysis.

- CONTRACTOR REPORT. Scientific and technical findings by NASA-sponsored contractors and grantees.

- CONFERENCE PUBLICATION. Collected papers from scientific and technical conferences, symposia, seminars, or other meetings sponsored or cosponsored by NASA.

- SPECIAL PUBLICATION. Scientific, technical, or historical information from NASA programs, projects, and mission, often concerned with subjects having substantial public interest.

- TECHNICAL TRANSLATION. English-language translations of foreign scientific and technical material pertinent to NASA's mission.

Specialized services that complement the STI Program Office's diverse offerings include creating custom thesauri, building customized databases, organizing and publishing research results…even providing videos.

For more information about the NASA STI Program Office, see the following:

- Access the NASA STI Program Home Page at ***http://www.sti.nasa.gov***

- E-mail your question via the Internet to help@sti.nasa.gov

- Fax your question to the NASA Access Help Desk at 301–621–0134

- Telephone the NASA Access Help Desk at 301–621–0390

- Write to:
  NASA Access Help Desk
  NASA Center for AeroSpace Information
  7121 Standard Drive
  Hanover, MD 21076–1320
  301–621–0390

NASA/TM—2005–213848

A "Kane's Dynamics" Model for the Active Rack Isolation System

Part Three: Addition of Umbilicals to the Nonlinear Model

J.K. Rupert
Dynetics, Inc., Huntsville, Alabama

R.D. Hampton
United States Military Academy, West Point, New York

G.S. Beech
Marshall Space Flight Center, Marshall Space Flight Center, Alabama

National Aeronautics and
Space Administration

Marshall Space Flight Center • MSFC, Alabama 35812

February 2005

TRADEMARKS

Trade names and trademarks are used in this report for identification only. This usage does not constitute an official endorsement, either expressed or implied, by the National Aeronautics and Space Administration.

Available from:

NASA Center for AeroSpace Information
7121 Standard Drive
Hanover, MD 21076–1320
301–621–0390

National Technical Information Service
5285 Port Royal Road
Springfield, VA 22161
703–487–4650

TABLE OF CONTENTS

LIST OF FIGURES

LIST OF FIGURES (Continued)

LIST OF ACRONYMS

ARIS	active rack isolation system
CAD	computer-aided design
ISPR	international standard payload rack
ISS	*International Space Station*
TM	Technical Memorandum

NOMENCLATURE

$\underline{x}$	vector of arbitrary quantity x
$\dot{x}$	first time derivative of arbitrary quantity x
$\hat{x}$	unit length of arbitrary quantity x
$\widehat{x}$	arbitrary reference frame x
$\tilde{x}$	arbitrary dynamical system x
${}_l x$	linearized arbitrary quantity x
x^*	arbitrary rigid-body x center of mass
x^T	transpose of matrix x
$\frac{d}{dt}$	ordinary (or total) derivative with respect to time t
$\frac{\partial}{\partial u}$	partial derivative with respect to scalar u
tr A	trace of arbitrary matrix A

Scalars

Uppercase

A_1^i	intersection point on ith actuator arm (fig. 2)
A_2^i	point locating ith upper stinger (fig. 2)
A_3^i	point locating ith Lorentz coil (fig. 2)
C	system damping matrix: lbf·s/ft
E	system disturbance input matrix

NOMENCLATURE (Continued)

F^{C_i}	magnitude of ith Lorentz coil force vector $\underline{F}^{C_i}$: lbf
F_i	point locating ith cross-flexure (fig. 2)
F_r	system holonomic generalized active force, for the rth generalized speed: ft·lbf
F_r^*	system holonomic generalized inertia force, for the rth generalized speed: ft·lbf
$\tilde{F}_r$	system nonholonomic generalized active force, for the rth generalized speed: ft·lbf
$\tilde{F}_r^*$	system nonholonomic generalized inertia force, for the rth generalized speed: ft·lbf
F_u	umbilical attachment point at the flotor end
F_{uh}	stator-fixed reference position of F_u
I	identity matrix
I_{jk}^{A/A^*}	central inertia scalar of rigid body A, for body-fixed coordinate directions $\hat{\underline{a}}_j$ and $\hat{\underline{a}}_k$: ft·lbf·s^2
K	system stiffness matrix: lbf/ft
M	system mass matrix: slug, lbf·s^2/ft
O	zero matrix
Q	rotation matrix from the $\hat{S}_i^1$ coordinate system to the $\hat{F}_i^1$ coordinate system
Q_{ij}	ijth element of rotation matrix Q
Q_r^B	contribution to the system holonomic generalized active force for the rth generalized speed, due to rigid body B: ft·lbf
$\left(Q_r^*\right)^B$	contribution to the system holonomic generalized inertia force for the rth generalized speed, due to rigid body B: ft·lbf
S_i	point locating ith lower stinger (fig. 2)
S_u	umbilical attachment point at the stator end

NOMENCLATURE (Continued)

$\tilde{S}$	total dynamical system (stator, flotor, actuators, umbilical)
X_{Fu}, Y_{Fu}, Z_{Fu}	geometric lengths: ft

Lowercase

a_j^i	geometric length for ith actuator assembly: ft
c_i	umbilical damping in the $\hat{\underline{\xi}}_i$ direction: lbf·s/ft
c_j^i	cosine of angle q_j for ith actuator assembly
f_j^i	geometric length for ith actuator assembly: ft
f_{jk}^i	rotation matrix element
g_i	direction cosines for $\hat{\underline{n}}_\phi$ in the $\hat{F}_1$ coordinate system
k_i	umbilical stiffness in the $\hat{\underline{\xi}}_i$ direction: lbf/ft
l_j^i	geometric length for ith actuator assembly: ft
m_A	mass of arbitrary rigid body A: slug, lbf·s^2/ft
p_2^i	geometric length for ith actuator assembly: ft
q_j^i	jth generalized coordinate for ith actuator: rad
r_{jk}	rotation matrix element
s_j^i	sine of angle q_j for ith actuator assembly
u_j^i	jth generalized speed for ith actuator: rad/s
v_j^i	geometric length for ith actuator assembly: ft
x_0, y_0, z_0	geometric lengths: ft

NOMENCLATURE (Continued)

x_i	umbilical elongation in the $\hat{\underline{\xi}}_i$ direction: ft
x_{Fu}, y_{Fu}, z_{Fu}	geometric lengths: ft
x_{Su}, y_{Su}, z_{Su}	geometric lengths: ft
κ_i	torsional umbilical stiffness about the $\hat{\underline{\xi}}_i$ axis: ft·lbf/rad
ϕ	flotor angle of twist relative to stator: rad
ϕ_i	angle-of-twist component in the $\hat{\underline{\xi}}_i$ direction: rad
γ_i	torsional umbilical damping about the $\hat{\underline{\xi}}_i$ axis: ft·lbf·s/rad

Vectors

Uppercase

$\underline{F}_b$	umbilical bias force in the reference position: lbf
$\underline{F}^{C_i}$	force exerted on the *i*th Lorentz coil by the flotor: lbf
$\underline{F}^{D}$	unknown disturbance force acting directly on the flotor: lbf
$\underline{F}^{F_i}$	force exerted on the flotor by the *i*th actuator arm: lbf
$\underline{F}^{U}$	force exerted on the flotor by the umbilical: lbf
$\underline{H}^{A/A^*}$	angular momentum of arbitrary rigid body A with respect to its mass center A^*: ft·lbf·s
$\underline{M}^{A_i}$	moment exerted on the *i*th actuator arm through the upper stinger, due to the *i*th pushrod: ft·lbf
$\underline{M}_b$	umbilical bias moment in the reference position: ft·lbf
$\underline{M}^{C_i}$	moment exerted on the *i*th Lorentz coil by the flotor, with $\underline{F}^{C_i}$ assumed to act at the *i*th cross flexure: ft·lbf

$\underline{M}^{D}$	unknown disturbance moment acting directly on the flotor, with $\underline{F}^{D}$ assumed to act at the flotor mass center: ft·lbf
$\underline{M}^{F_i}$	moment exerted on the flotor by the ith actuator, with $\underline{F}^{F_i}$ assumed to act at the ith cross-flexure: ft·lbf

Lowercase

${}^{A}\underline{a}^{B}$	acceleration of arbitrary point B, with arbitrary reference frame A assumed fixed: ft/s^2
$\underline{a}^{I}$	translational acceleration of stator (due to g-jitter): ft/s^2
$\underline{d}$	system disturbance vector: lbf and ft·lbf elements
$\underline{i}$	system control current vector: amp
$\hat{\underline{n}}_{\phi}$	unit vector in direction of rotation axis for stator-to-flotor rotation $\phi\,\hat{\underline{n}}_{\phi}$
$\underline{q}$	Vector of generalized coordinates: rad
$\underline{r}^{AB}$	position vector from arbitrary point A to arbitrary point B: ft
$\underline{u}$	vector of generalized speeds: rad/s
$\underline{u}^{I}$	vector of independent generalized speeds: rad/s
${}^{A}\underline{v}^{B}$	velocity of arbitrary point B, with arbitrary reference frame A assumed fixed: ft/s
${}^{A}\underline{\alpha}^{B}$	angular acceleration of arbitrary reference frame B with respect to arbitrary reference frame A: rad/s^2
${}^{A}\underline{\omega}^{B}$	angular velocity of arbitrary reference frame B with respect to arbitrary reference frame A: rad/s

TECHNICAL MEMORANDUM

A "KANE'S DYNAMICS" MODEL FOR THE ACTIVE RACK ISOLATION SYSTEM

PART THREE: ADDITION OF UMBILICALS TO THE NONLINEAR MODEL

1. INTRODUCTION

As the only active rack-level isolation system for the *International Space Station (ISS)*, the active rack isolation system (ARIS) is the central component of the stationwide strategy to meet *ISS* isolation requirements.[1] It serves to attenuate the various disturbances that unavoidably accompany manned space flight. Umbilicals, as shown in figure 1, are to be used in support of many experiments planned for space, providing services such as cooling, power, vacuum, and data transmission. ARIS is nominally equipped with thirteen umbilicals.[1]

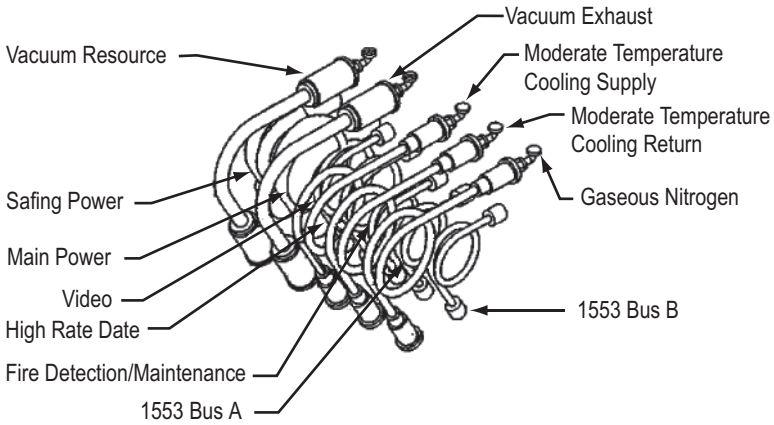

Figure 1. Detailed diagram of the umbilical assembly.

Unfortunately, the ARIS umbilicals are not only the primary transmitters of indirect; i.e., off-board, disturbances from *ISS* to the international standard payload rack (ISPR), they are also typically nonlinear, hysteretic, and poorly characterized.[2] Since the respective umbilicals are attached at different locations to *ISS* at the bottom plate and to the base of the ISPR at the z-panel, it is desirable to include this attachment-point information as part of the ARIS model to improve model fidelity and reduce the amount of uncertainty for which the controller must compensate.

In part one of this series, NASA/TM—2001–211063, a high-fidelity, linearized, analytical model of ARIS was derived using traditional, hand-calculation methods.[3] The model was developed directly, using Thomas Kane's method, without intermediate development of the full nonlinear model.[4] Part one briefly outlined an approach for incorporating an ARIS umbilical into the model, using diagonalized stiffness and damping matrices.

Part two, NASA/TM—2004–213552, presented four computer-based, numerical models of ARIS, one of which was purely kinematical, and the remaining three, dynamical.[5] These numerical models were used collectively to verify and simplify the linearized analytical model developed in part one.

This Technical Memorandum (TM) completes the nonlinear ARIS model of part two, by adding multiple Hookean umbilicals with full stiffness and damping matrices. Comparisons against simple single-degree-of-freedom truth models indicate that the completed nonlinear model has input responses that follow those expected given the laws of physics.

This TM (1) briefly summarizes the existing Kane's model, (2) describes the addition of an arbitrary number of massless umbilicals with specified arbitrary attachment points and arbitrary (parallel) stiffness and dampings, to that model, (3) provides a brief description of Autolev™ in which the underlying untethered model was developed, and (4) presents the process by which verification of the enhanced model was accomplished along with some verification results.

To develop the enhanced model, it was assumed that the umbilicals were to be included individually in the model, rather than as a combined, or effective, umbilical. For the sake of simplicity and since the range of motion is small, each umbilical is assumed to be Hookean and massless since an algebraic state-space model, one that is useful for controller design using state-space-based methods, is desired. Also, each is modeled as a three-dimensional (six-by-six, constant) stiffness matrix in parallel with a three-dimensional (six-by-six, constant) damping matrix.

In the verification stage, the model of the tethered ARIS system is compared with two baseline, or truth, models. One truth model consists of a translational, one-dimensional, second-order spring-mass-damper system, and the other consists of a corresponding rotational system.[6] The verification checks indicate that the proposed Kane's model, when properly calibrated against experimental data, will provide a high-fidelity representation of ARIS for simulation and controller-design purposes.

2. COORDINATE SYSTEMS

The coordinate systems, generalized coordinates, generalized speeds, and angular velocities used for the Kane's model were presented previously in part one.[3,7,8] They are reviewed in this section and in sections 3 and 4 for the reader's convenience.

With the ISPR (flotor) in the reference position; i.e., centered in its *ISS*-fixed rattle space, fix eight right-handed, orthogonal coordinate systems in the ISPR, one at each of the cross-flexure centers (fig. 2). Let the *i*th coordinate system have origin F_i, located at the center of the *i*th cross flexure, (*i*=1,…,8), with axis directions determined by an orthonormal set of unit vectors, $\hat{\underline{f}}^i_j$ (*j*=1,2,3). The overhat indicates unit length, the index, *i*, corresponds to the *i*th actuator assembly, and the index, *j*, distinguishes the three vectors. Orient the unit vectors such that $\hat{\underline{f}}^i_2$ is along the *i*th arm, toward the *i*th voice coil; $\hat{\underline{f}}^i_1$ is directed parallel to the other segment of the *i*th arm and toward the upper stinger, which is located at A^i_2; and $\hat{\underline{f}}^i_3$ is in the direction $\hat{\underline{f}}^i_1 \times \hat{\underline{f}}^i_2$ along the intersection of the two crosspieces of the *i*th cross flexure.

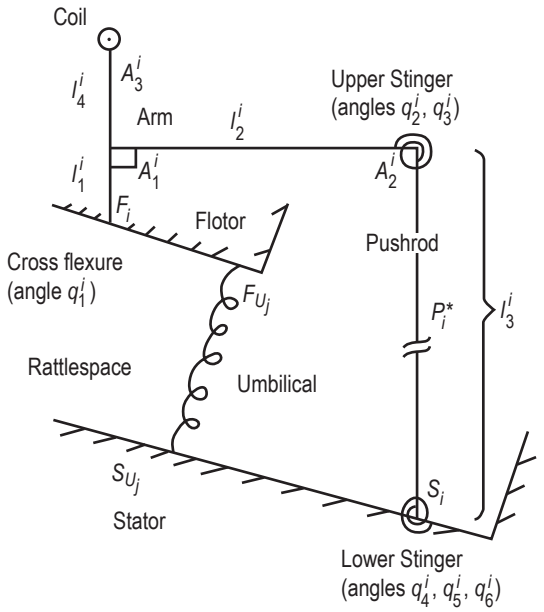

Figure 2. Kinematic diagram, including the *i*th actuator assembly and the umbilical.

Fix a similar right-handed coordinate system, $\hat{\underline{\alpha}}_j^i$($j$=1,2,3), in the arm of each actuator. Locate each system, $\hat{\underline{\alpha}}_j^i$, such that it is coincident with the corresponding flotor-fixed coordinate system, $\hat{\underline{f}}_j^i$, when the flotor is in the reference position.

Locate eight more arm-fixed coordinate systems, described by $\hat{\underline{a}}_j^i$, at the respective upper stingers, points A_2^i. At the respective lower stingers, points S_i, place eight pushrod-fixed coordinate systems $\hat{\underline{p}}_j^i$, and eight stator-fixed (*ISS*-fixed) coordinate systems, $\hat{\underline{s}}_j^i$. Orient these 24 coordinate systems such that when the stingers are relaxed; i.e., with the flotor in the reference position, the coordinate directions, $\hat{\underline{a}}_j^i$, $\hat{\underline{p}}_j^i$, and $\hat{\underline{s}}_j^i$, are coaligned for the ith actuator, with $\hat{\underline{p}}_2^i$ (along with $\hat{\underline{a}}_2^i$ and $\hat{\underline{s}}_2^i$, in the reference position) directed from S_i towards A_2^i. Directions $\hat{\underline{p}}_1^i$ and $\hat{\underline{p}}_3^i$ (in the reference position) are determined by fixed rotation matrices relating the $\hat{\underline{a}}_j^i$ to the $\hat{\underline{\alpha}}_j^i$ coordinate systems.

Finally, define a primary, central, flotor-fixed, reference coordinate system with coordinate directions, $\hat{\underline{f}}_j$. All other flotor-fixed coordinate systems, $\hat{\underline{f}}_j^i$, are assumed capable of being referenced; e.g., by known direction cosine angles, to this system.

Define a stator-fixed coordinate system, $\hat{\underline{\xi}}_i^j$, that is associated with the jth umbilical. Define the rotation matrix from the stator-fixed coordinate system, $\hat{\underline{s}}_i^1$, to the new coordinate system, $\hat{\underline{\xi}}_i^j$, by

$$\begin{Bmatrix} \hat{\underline{\xi}}_1^j \\ \hat{\underline{\xi}}_2^j \\ \hat{\underline{\xi}}_3^j \end{Bmatrix} = \left[\Re_j \right] \begin{Bmatrix} \hat{\underline{s}}_1^1 \\ \hat{\underline{s}}_2^1 \\ \hat{\underline{s}}_3^1 \end{Bmatrix}, \tag{1}$$

where

$$\left[\Re_j \right] = \begin{bmatrix} r_{11}^j & r_{12}^j & r_{13}^j \\ r_{21}^j & r_{22}^j & r_{23}^j \\ r_{31}^j & r_{32}^j & r_{33}^j \end{bmatrix}. \tag{2}$$

Note that $\left[\Re_j \right]$ is a constant matrix, and it could differ for different umbilical circumstances.

3. GENERALIZED COORDINATES AND GENERALIZED SPEEDS

Let the $\underline{\hat{\alpha}}_j^i$ coordinate system rotate, relative to the $\underline{\hat{f}}_j^i$ coordinate system, through the positive angle, q_1^i, about the $\underline{\hat{f}}_3^i$ axis against the cross-flexure stiffness, k_1^i. Similarly, let the orientation of the $\underline{\hat{a}}_j^i$ coordinate system, relative to the $\underline{\hat{p}}_j^i$ coordinate system, be described by consecutive positive rotations— q_2^i about the $\underline{\hat{p}}_1^i$ axis and q_3^i about the moved 3 axis. Also, let the orientation of the $\underline{\hat{p}}_j^i$ coordinate system, relative to the $\underline{\hat{s}}_j^i$ coordinate system, be described by consecutive positive rotations— q_4^i about the $\underline{\hat{s}}_3^i$ axis, q_5^i about the moved 2 axis, and q_6^i about the moved 1 axis. The six generalized speeds are defined as the time rates of change of the respective generalized coordinates:

$$u_j^i = \dot{q}_j^i \left(i = 1, \cdots, 8; j = 1, \cdots, 6 \right) . \tag{3}$$

Finally, let c_j^i and s_j^i represent the cosines and sines of the respective angles, q_j^i.

4. ANGULAR VELOCITIES OF REFERENCE FRAMES AND RIGID BODIES

Designate the reference frames corresponding to the stator, the *i*th pushrod, the *i*th arm, and the flotor, as the symbols $\widehat{S}$, $\widehat{P}_i$, $\widehat{A}_i$, and $\widehat{F}$, respectively. Let $\widehat{S}_i$ and $\widehat{F}_i$ represent, respectively, the coordinate systems in $\widehat{S}$ and $\widehat{F}$, respectively defined by $\left[\begin{array}{ccc}\hat{\underline{s}}_1^i & \hat{\underline{s}}_2^i & \hat{\underline{s}}_3^i\end{array}\right]^T$ and $\left[\begin{array}{ccc}\hat{\underline{f}}_1^i & \hat{\underline{f}}_2^i & \hat{\underline{f}}_3^i\end{array}\right]^T$. Two intermediate reference frames were introduced previously to permit describing the angular velocity of each pushrod relative to the stator. Designate those intermediate frames corresponding to the *i*th actuator assembly as $\widehat{R}_i$ and $\widehat{Q}_i$. Another intermediate reference frame was previously introduced between frames $\widehat{P}_i$ and $\widehat{A}_i$; designate that frame as $\widehat{T}_i$. Finally, designate the stator-fixed reference frame corresponding to the *j*th umbilical as $\widehat{\Xi}_j$.

Let each intermediate reference frame have a frame-fixed, dextral set of unit vectors. Indicate the unit vectors for each of these frame-fixed coordinate systems by using the corresponding lowercase letter; i.e., $\hat{\underline{r}}_j^i$ corresponding to $\widehat{R}_i$, etc. The following gives the expressions for the angular velocities of the various reference frames and rigid bodies of $\tilde{S}$:

$$^{F_i}\underline{\omega}^{A_i} = u_1^i \hat{\underline{f}}_3^i \ , \tag{4}$$

$$^{P_i}\underline{\omega}^{T_i} = u_2^i \hat{\underline{p}}_1^i \ , \tag{5}$$

$$^{T_i}\underline{\omega}^{A_i} = u_3^i \hat{\underline{t}}_3^i \ , \tag{6}$$

$$^{S_i}\underline{\omega}^{R_i} = u_4^i \hat{\underline{s}}_3^i \ , \tag{7}$$

$$^{R_i}\underline{\omega}^{Q_i} = u_5^i \hat{\underline{r}}_2^i \ , \tag{8}$$

and

$$^{Q_i}\underline{\omega}^{P_i} = u_6^i \hat{\underline{q}}_1^i \ . \tag{9}$$

Using the addition theorem for angular velocities, the angular velocities of the rigid bodies of $\tilde{S}$ are

$$^{S_i}\underline{\omega}^{A_i} = u_2^i \hat{\underline{p}}_1^i + u_3^i \hat{\underline{t}}_3^i + u_4^i \hat{\underline{s}}_3^i + u_5^i \hat{\underline{r}}_2^i + u_6^i \hat{\underline{q}}_1^i \ , \tag{10}$$

$$ {}^{S_i}\underline{\omega}^{P_i} = u_4^i \underline{\hat{s}}_3^i + u_5^i \underline{\hat{r}}_2^i + u_6^i \underline{\hat{q}}_1^i \ , \tag{11} $$

and

$$ {}^{S_i}\underline{\omega}^{F_i} = u_4^i \underline{\hat{s}}_3^i + u_5^i \underline{\hat{r}}_2^i + u_6^i \underline{\hat{q}}_1^i \ . \tag{12} $$

5. GENERALIZED ACTIVE FORCE CONTRIBUTIONS DUE TO THE UMBILICALS

5.1 Generalized Active Force Equations

Equations of motion developed using Kane's method consist of contributions called generalized active forces (GAFs), related to system forces and moments, and contributions called generalized inertia forces (GIFs), related to the time derivatives of linear and angular momenta.[4] For ARIS, the development of the GAF and GIF contributions due to the actuator arms and pushrods, the flotor, and a single umbilical with diagonal stiffness and damping matrices is detailed in part one.[3] Because the umbilicals are assumed to be massless, they make no contributions to the GIFs, and thus, they contribute only to the GAFs.

In previous treatments (part one of this series and a paper by Rupert and Hampton), the umbilical stiffness and damping matrices were assumed to be diagonal with no coupling between translation and rotation, or between axes.[3,8] However, coupling will always exist between translation and rotation and typically between axes as well.[2,9] In other words, for an arbitrary set of orthonormal axes, one expects that the six-by-six umbilical stiffness and damping matrices will be full. Consequently, full matrices are assumed in the following treatment.

Designate the *r*th partial velocity of the *j*th umbilical's flotor-attachment point (with reference frame $\widehat{S}$ assumed to be fixed, for purposes of differentiation) as ${}^{S_1}\underline{v}_r^{F_{Uj}}$ and the *r*th partial angular velocity of the flotor relative to the stator as ${}^{S}\underline{\omega}_r^{F}$. Designate the force and moment that the *j*th umbilical exerts on the flotor as $\underline{F}^{Uj}$ and $\underline{M}^{Uj}$, respectively, where the force is assumed to act on the flotor at the *j*th umbilical attachment point F_{Uj}. Let all direct disturbance forces and moments that are exerted on the flotor—such as those due to air currents, to direct contact by astronauts, or to moving parts on flotor-mounted experiments—be designated collectively by the respective symbols $\underline{F}^{D}$ and $\underline{M}^{D}$. Finally, let $-\underline{F}^{Ci}$ and $-\underline{M}^{Ci}$ represent, respectively, the force and moment exerted by the *i*th Lorentz coil, located at A_3^i, on the flotor, where

$$\underline{F}^{Ci} = F^{Ci}\,\hat{\underline{a}}_1^i \ , \tag{13}$$

assumed to act at point F_i and

$$\underline{M}^{Ci} = \underline{r}^{F_i A_3^i} \times \underline{F}^{Ci} = -F^{Ci}(l_1^i + l_4^i)\hat{\underline{a}}_3^i \ . \tag{14}$$

Then, assuming a nominal complement of 13 umbilicals, the GAF contribution due to the flotor, for the *r*th generalized speed, can be written as

$$Q_r^F \coloneqq \sum_{j=1}^{13}\left({}^{S_1}\underline{v}_r^{F_{U_j}} \cdot \underline{F}^{U_j} + {}^{S}\underline{\omega}_r^{F} \cdot \underline{M}^{U_j} \right) + {}^{S}\underline{\omega}_r^{F} \cdot \left(\underline{M}^{D} + \sum_{i=1}^{8} k_1^i q^i {}_1\underline{\hat{f}}_3^i \right)$$
$$+ {}^{S_1}\underline{v}_r^{F^*} \cdot \underline{F}^{D} - \sum^{8}\left({}^{S_1}\underline{v}_r^{F_i} \cdot \underline{F}^{C_i} + {}^{S_1}\underline{\omega}_r^{F} \cdot \underline{M}^{C_i} \right) \ . \tag{15}$$

The *j*th umbilical affects only the first two terms, with the contribution

$${}^{j}Q_r^F \coloneqq {}^{S_1}\underline{v}_r^{F_{U_j}} \cdot \underline{F}^{U_j} + {}^{S}\underline{\omega}_r^{F} \cdot \underline{M}^{U_j} \ . \tag{16}$$

These two terms will be treated in sections 5.2 and 5.3.

5.2 Partial Velocities ${}^{S_1}\underline{v}_r^{F_{U_j}}$

Represent by $\underline{r}^{AB}$ the position vector from arbitrary point A to arbitrary point B, and define the following position vectors using the indicated scalars:

$$\underline{r}^{F_i A_2^i} = l_1^i \underline{\hat{a}}_2^i + l_2^i \underline{\hat{a}}_1^i \ , \tag{17}$$

$$\underline{r}^{S_i A_2^i} = l_3^i \underline{\hat{p}}_2^i \ , \tag{18}$$

$$\underline{r}^{S_i P_i^*} = p_2^i \underline{\hat{p}}_2^i \ , \tag{19}$$

$$\underline{r}^{A_2^i A_i^*} = a_1^i \underline{\hat{a}}_1^i + a_2^i \underline{\hat{a}}_2^i \ , \tag{20}$$

and

$$\underline{r}^{F_i F^*} = f_1^i \underline{\hat{f}}_1^i + f_2^i \underline{\hat{f}}_2^i + f_3^i \underline{\hat{f}}_3^i \ . \tag{21}$$

Represent the position vector from the flotor center of mass to the *j*th umbilical's flotor-attachment point as

$$\underline{r}^{F^* F_{U_j}} = X_{F_U}^j \underline{\hat{f}}_1^1 + Y_{F_U}^j \underline{\hat{f}}_2^1 + Z_{F_U}^j \underline{\hat{f}}_3^1 \tag{22}$$

for appropriately defined measure numbers. Then, referring to figure 2, the position vector from the first-lower-stinger attachment point to the flotor center of mass is seen to be

$$\underline{r}^{S_1 F^*} = l_3^1 \underline{\hat{p}}_2^1 - l_1^1 \underline{\hat{a}}_2^1 - l_2^1 \underline{\hat{a}}_1^1 + f_1^1 \underline{\hat{f}}_1^1 + f_2^1 \underline{\hat{f}}_2^1 + f_3^1 \underline{\hat{f}}_3^1 \ . \tag{23}$$

Since

$$\underline{r}^{S_1 F_{U_j}} = \underline{r}^{S_1 F^*} + \underline{r}^{F^* F_{U_j}} \quad , \tag{24}$$

the rth partial velocity of the flotor-attachment point F_{U_j} is[6]

$$ {}^{S_1}\underline{v}_r^{F_{U_j}} = {}^{S_1}\underline{v}_r^{F^*} + \left[\frac{\partial}{\partial u_r} \left({}^{S_1}\underline{\omega}^{F_1} \times \underline{r}^{F^* F_{U_j}} \right) \right] . \tag{25}$$

The position vectors $\underline{r}^{S_1 F^*}$ and $\underline{r}^{F^* F_{U_j}}$, and the angular velocity vector ${}^{S_1}\underline{\omega}^{F_1}$, can be expressed in terms of the coordinates, q_j^1 (j=1,…,6), and the associated generalized speeds of actuator number 1. This means that the velocity of each attachment point, F_{U_j}, can be expressed in terms of these same coordinates and generalized speeds so that the partial velocities defined in equation (25) are nonzero for only those six generalized speeds; i.e., for r=1,…,6.

Expanding equation (25) in terms of the jth stator-fixed coordinate system, $\hat{\underline{\xi}}_i^j$, (associated with the jth umbilical) and collecting terms, the rth partial velocity for F_{U_j} can be expressed as

$$ {}^{S_1}\underline{v}_r^{F_{U_j}} = \sum_{i=1}^{3} v_{ri}^{U_j} \, \hat{\underline{\xi}}_i^j \quad , \tag{26}$$

where the scalars, $v_{ri}^{U_j}$, are simply the measure numbers in analytical (algebraic) form. In matrix form, the six nonzero partial velocities for the jth umbilical's flotor-attachment point are

$$\begin{Bmatrix} {}^{S_1}\underline{v}_1^{F_{U_j}} \\ {}^{S_1}\underline{v}_2^{F_{U_j}} \\ {}^{S_1}\underline{v}_3^{F_{U_j}} \\ {}^{S_1}\underline{v}_4^{F_{U_j}} \\ {}^{S_1}\underline{v}_5^{F_{U_j}} \\ {}^{S_1}\underline{v}_6^{F_{U_j}} \end{Bmatrix} = \begin{Bmatrix} \sum_{i=1}^{3} v_{1i}^{U_j} \, \hat{\underline{\xi}}_i^j \\ \sum_{i=1}^{3} v_{2i}^{U_j} \, \hat{\underline{\xi}}_i^j \\ \sum_{i=1}^{3} v_{3i}^{U_j} \, \hat{\underline{\xi}}_i^j \\ \sum_{i=1}^{3} v_{4i}^{U_j} \, \hat{\underline{\xi}}_i^j \\ \sum_{i=1}^{3} v_{5i}^{U_j} \, \hat{\underline{\xi}}_i^j \\ \sum_{i=1}^{3} v_{6i}^{U_j} \, \hat{\underline{\xi}}_i^j \end{Bmatrix} = \begin{bmatrix} v_{11}^{U_j} & v_{12}^{U_j} & v_{13}^{U_j} \\ v_{21}^{U_j} & v_{22}^{U_j} & v_{23}^{U_j} \\ v_{31}^{U_j} & v_{32}^{U_j} & v_{33}^{U_j} \\ v_{41}^{U_j} & v_{42}^{U_j} & v_{43}^{U_j} \\ v_{51}^{U_j} & v_{52}^{U_j} & v_{53}^{U_j} \\ v_{61}^{U_j} & v_{62}^{U_j} & v_{63}^{U_j} \end{bmatrix} \begin{Bmatrix} \hat{\underline{\xi}}_1^j \\ \hat{\underline{\xi}}_2^j \\ \hat{\underline{\xi}}_3^j \end{Bmatrix} . \tag{27}$$

5.3 Partial Angular Velocities ${}^{S_1}\underline{\omega}_r^{F_1}$

From equation (12), the angular velocity of the flotor relative to the stator can be expressed as

$$ {}^{S_1}\underline{\omega}^{F_1} = u_2^1 \hat{\underline{p}}_1^1 + u_3^1 \hat{\underline{t}}_3^1 + u_4^1 \hat{\underline{s}}_3^1 + u_5^1 \hat{\underline{r}}_2^1 + u_6^1 \hat{\underline{q}}_1^1 - u_1^1 \hat{\underline{f}}_3^1 \ . \tag{28} $$

Following the procedure and using a notation analogous to that of the previous subsection, the nonzero partial angular velocities can be expressed in the matrix form,

$$ \begin{Bmatrix} {}^{S_1}\underline{\omega}_1^F \\ {}^{S_1}\underline{\omega}_2^F \\ {}^{S_1}\underline{\omega}_3^F \\ {}^{S_1}\underline{\omega}_4^F \\ {}^{S_1}\underline{\omega}_5^F \\ {}^{S_1}\underline{\omega}_6^F \end{Bmatrix} = \begin{Bmatrix} \sum_{i=1}^{3} \omega_{1i}^{U_j} \hat{\underline{\xi}}_i^j \\ \sum_{i=1}^{3} \omega_{2i}^{U_j} \hat{\underline{\xi}}_i^j \\ \sum_{i=1}^{3} \omega_{3i}^{U_j} \hat{\underline{\xi}}_i^j \\ \sum_{i=1}^{3} \omega_{4i}^{U_j} \hat{\underline{\xi}}_i^j \\ \sum_{i=1}^{3} \omega_{5i}^{U_j} \hat{\underline{\xi}}_i^j \\ \sum_{i=1}^{3} \omega_{6i}^{U_j} \hat{\underline{\xi}}_i^j \end{Bmatrix} = \begin{bmatrix} \omega_{11}^{U_j} & \omega_{12}^{U_j} & \omega_{13}^{U_j} \\ \omega_{21}^{U_j} & \omega_{22}^{U_j} & \omega_{23}^{U_j} \\ \omega_{31}^{U_j} & \omega_{32}^{U_j} & \omega_{33}^{U_j} \\ \omega_{41}^{U_j} & \omega_{42}^{U_j} & \omega_{43}^{U_j} \\ \omega_{51}^{U_j} & \omega_{52}^{U_j} & \omega_{53}^{U_j} \\ \omega_{61}^{U_j} & \omega_{62}^{U_j} & \omega_{63}^{U_j} \end{bmatrix} \begin{Bmatrix} \hat{\underline{\xi}}_1^j \\ \hat{\underline{\xi}}_2^j \\ \hat{\underline{\xi}}_3^j \end{Bmatrix} . \tag{29} $$

5.4 General Form for Umbilical Forces and Moments

With full stiffness and damping matrices, the *j*th-umbilical force, $\underline{F}^{U_j}$, and moment, $\underline{M}^{U_j}$, will each be expressed in terms of umbilical-elongation-, elongation-rate-, angle-of-twist-, and twist-rate-component measure numbers. In vector form, the umbilical elongation is $\underline{r}^{F_{Uh_j}F_{U_j}}$, where F_{Uh_j} designates the stator-fixed location of the umbilical attachment point, F_{U_j}, in the reference position. Let $\phi\hat{\underline{n}}_\phi$ represent, in vector form, the rotation of the flotor, relative to the stator, from the reference position. The term $\hat{\underline{n}}_\phi$ is in the positive direction of the rotation axis, and ϕ is the positive angle of twist about that axis. Then, for the *j*th umbilical, the elongations; i.e., the elongation measure numbers, are

$$ x_i^j = \underline{r}^{F_{Uh_j}F_{U_j}} \cdot \hat{\underline{\xi}}_i^j \ , \tag{30} $$

the elongation rates are $\dot{x}_i^j$, the angles of twist are

$$\phi_i^j = \phi \hat{\underline{n}}_\phi \cdot \hat{\underline{\xi}}_i^j \quad , \tag{31}$$

and the twist rates are $\dot{\phi}_i^j$.

Let the bias force and moment exerted on the flotor by the *j*th umbilical be $\underline{F}_b^{U_j}$ and $\underline{M}_b^{U_j}$, respectively. Next, for *i*=1,2,3, define

$$F_{bi}^{U_j} = \underline{F}_b^{U_j} \cdot \hat{\underline{\xi}}_i^j \quad , \tag{32}$$

$$M_{bi}^{U_j} = \underline{M}_b^{U_j} \cdot \hat{\underline{\xi}}_i^j \quad , \tag{33}$$

$$F_i^{U_j} = \underline{F}^{U_j} \cdot \hat{\underline{\xi}}_i^j \quad , \tag{34}$$

and

$$M_i^{U_j} = \underline{M}^{U_j} \cdot \hat{\underline{\xi}}_i^j \quad . \tag{35}$$

Then, in matrix form, the combined force and moment equations are as follows:

$$\begin{Bmatrix} F_1^{U_j} \\ F_2^{U_j} \\ F_3^{U_j} \\ M_1^{U_j} \\ M_2^{U_j} \\ M_3^{U_j} \end{Bmatrix} = \underbrace{\begin{bmatrix} k_{11}^{U_j} & \cdots & k_{16}^{U_j} \\ \vdots & \ddots & \vdots \\ k_{61}^{U_j} & \cdots & k_{66}^{U_j} \end{bmatrix}}_{K} \begin{Bmatrix} x_1^{U_j} \\ x_2^{U_j} \\ x_3^{U_j} \\ \phi_1^{U_j} \\ \phi_2^{U_j} \\ \phi_3^{U_j} \end{Bmatrix} + \underbrace{\begin{bmatrix} c_{11}^{U_j} & \cdots & c_{16}^{U_j} \\ \vdots & \ddots & \vdots \\ c_{61}^{U_j} & \cdots & c_{66}^{U_j} \end{bmatrix}}_{C} \begin{Bmatrix} \dot{x}_1^{U_j} \\ \dot{x}_2^{U_j} \\ \dot{x}_3^{U_j} \\ \dot{\phi}_1^{U_j} \\ \dot{\phi}_2^{U_j} \\ \dot{\phi}_3^{U_j} \end{Bmatrix} + \begin{Bmatrix} F_{b1}^{U_j} \\ F_{b2}^{U_j} \\ F_{b3}^{U_j} \\ M_{b1}^{U_j} \\ M_{b2}^{U_j} \\ M_{b3}^{U_j} \end{Bmatrix} , \tag{36}$$

where the stiffness and damping elements, obtained by measurements or other means, and the stiffness and damping matrices are indicated by the designations *k*, *c*, *K*, and *C*, respectively. The stiffness and damping element superscripts and subscripts have their obvious meanings. To use the left-hand elements of equation (36) in equation (16), these elongations and angles of twist, along with their rates, must now be reexpressed in terms of the system coordinates and generalized speeds.

5.5 Umbilical Elongations and Elongation Rates

Recall equation (30), for *i*=1,2,3; but

$$\underline{r}^{F_{Uh_j} F_{U_j}} = \underline{r}^{S_1 F_1} + \underline{r}^{F_1 F_{U_j}} - \underline{r}^{S_1 S_{U_j}} - \underline{r}^{S_{U_j} F_{Uh_j}} \quad , \tag{37}$$

where the right-hand-side terms can be expressed by

$$\underline{r}^{S_1F_1} = l_3^1 \underline{\hat{p}}_2^1 - l_2^1 \underline{\hat{a}}_1^1 - l_1^1 \underline{\hat{a}}_2^1 \ , \tag{38}$$

$$\underline{r}^{F_1F_{U_j}} = x_{F_U}^j \underline{\hat{f}}_1^1 + y_{F_U}^j \underline{\hat{f}}_2^1 + z_{F_U}^j \underline{\hat{f}}_3^1 \ , \tag{39}$$

$$\underline{r}^{S_1S_{U_j}} = x_{S_U}^j \underline{\hat{s}}_1^1 + y_{S_U}^j \underline{\hat{s}}_2^1 + z_{S_U}^j \underline{\hat{s}}_3^1 \ , \tag{40}$$

and

$$\underline{r}^{S_{U_j}F_{Uh_j}} = x_0^j \underline{\hat{s}}_1^1 + y_0^j \underline{\hat{s}}_2^1 + z_0^j \underline{\hat{s}}_3^1 \tag{41}$$

for appropriately defined coefficients.

Using equation (1), equation (37) can now be written in terms of the $\underline{\hat{\xi}}_i^j$ coordinate system in linearized form

$$\underline{r}^{F_{Uh_j}F_{U_j}} = x_1^j \underline{\hat{\xi}}_1^j + x_2^j \underline{\hat{\xi}}_2^j + x_3^j \underline{\hat{\xi}}_3^j \ , \tag{42}$$

where

$$\begin{Bmatrix} x_1^j \\ x_2^j \\ x_3^j \end{Bmatrix} = \left[\Re_j\right] \cdot \begin{Bmatrix} C_1^j + y_{F_U}^j \left(q_1^1 - q_3^1 - q_4^1\right) + z_{F_U}^j q_5^1 - l_3^1 q_4^1 + l_1^1 \left(q_3^1 + q_4^1\right) \\ C_2^j - z_{F_U}^j \left(q_2^1 + q_6^1\right) - x_{F_U}^j \left(q_1^1 - q_3^1 - q_4^1\right) - l_2^1 \left(q_3^1 + q_4^1\right) \\ C_3^j + \left(l_2^1 - x_{F_U}^j\right) q_5^1 + \left(y_{F_U}^j - l_1^1\right)\left(q_2^1 + q_6^1\right) + l_3^1 q_6^1 \end{Bmatrix} \tag{43}$$

for

$$C_1^j = x_{F_U}^j - x_{S_U}^j - l_2^1 - x_0^j \ , \tag{44}$$

$$C_2^j = y_{F_U}^j - y_{S_U}^j + l_3^1 - l_1^1 - y_0^j \ , \tag{45}$$

and

$$C_3^j = z_{F_U}^j - z_{S_U}^j - z_0^j \ . \tag{46}$$

Differentiating equation (43),[6]

$$\begin{Bmatrix} \dot{x}_1^j \\ \dot{x}_2^j \\ \dot{x}_3^j \end{Bmatrix} = \left[\Re_j\right] \cdot \begin{Bmatrix} y_{F_U}^j \left(u_1^1 - u_3^1 - u_4^1\right) + z_{F_U}^j u_5^1 - l_3^1 u_4^1 + l_1^1 \left(u_3^1 + u_4^1\right) \\ -z_{F_U}^j \left(u_2^1 + u_6^1\right) - x_{F_U}^j \left(u_1^1 - u_3^1 - u_4^1\right) - l_2^1 \left(u_3^1 + u_4^1\right) \\ \left(l_2^1 - x_{F_U}^j\right) u_5^1 + \left(y_{F_U}^j - l_1^1\right)\left(u_2^1 + u_6^1\right) + l_3^1 u_6^1 \end{Bmatrix} . \tag{47}$$

Equations (43) and (47) give the umbilical elongations and elongation rates in terms of the six independent generalized speeds. It is now required to do the same for the umbilical angles and angles of twist.

5.6 Umbilical Angles of Twist and Twist Rates

Express $\underline{\hat{n}}_\phi$ as

$$\underline{\hat{n}}_\phi = g_1 \underline{\hat{s}}_1^1 + g_2 \underline{\hat{s}}_2^1 + g_3 \underline{\hat{s}}_3^1 \ . \tag{48}$$

Define rotation matrix Q by

$$\begin{Bmatrix} \underline{\hat{f}}_1^1 \\ \underline{\hat{f}}_2^1 \\ \underline{\hat{f}}_3^1 \end{Bmatrix} = [Q] \begin{Bmatrix} \underline{\hat{s}}_1^1 \\ \underline{\hat{s}}_2^1 \\ \underline{\hat{s}}_3^1 \end{Bmatrix} , \tag{49}$$

and then the linearized three-by-three rotation matrix, ${}_lQ$, has elements, ${}_lQ_{ij}$, defined as

$$\begin{Bmatrix} \underline{\hat{f}}_1^1 \\ \underline{\hat{f}}_2^1 \\ \underline{\hat{f}}_3^1 \end{Bmatrix} = \begin{bmatrix} 1 & -q_1^1 + q_3^1 + q_4^1 & -q_5^1 \\ q_1^1 - q_3^1 - q_4^1 & 1 & q_2^1 + q_6^1 \\ q_5^1 & -q_2^1 - q_6^1 & 1 \end{bmatrix} \begin{Bmatrix} \underline{\hat{s}}_1^1 \\ \underline{\hat{s}}_2^1 \\ \underline{\hat{s}}_3^1 \end{Bmatrix} . \tag{50}$$

Let the postsuperscript T indicate matrix transposition and let tr ${}_lQ$ represent the trace of ${}_lQ$. For small angles it can be shown that[10]

$$\phi \begin{bmatrix} 0 & g_3 & -g_2 \\ -g_3 & 0 & g_1 \\ g_2 & -g_1 & 0 \end{bmatrix} = \frac{{}_lQ - {}_lQ^T}{\left(1 + \mathrm{tr}\, {}_lQ\right)^{1/2}} \ . \tag{51}$$

Substitution for ${}_lQ$, as defined in equation (50), into equation (51) and simplification yield

$$g_1 = \frac{1}{\phi} \cdot \left(q_2^1 + q_6^1 \right) , \tag{52}$$

$$g_2 = \frac{1}{\phi} \cdot q_5^1 , \tag{53}$$

and

$$g_3 = -\frac{1}{\phi} \cdot \left(q_1^1 - q_3^1 - q_4^1 \right) . \tag{54}$$

Substituting from equations (52)–(54) into equation (48) and transforming into the $\hat{\underline{s}}_i^1$ coordinate systems by use of ${}_lQ$ yield the following linearized expression for the flotor rotation:

$$\phi \, \hat{\underline{n}}_\phi = \left(q_2^1 + q_6^1 \right) \hat{\underline{s}}_1^1 + q_5^1 \, \hat{\underline{s}}_2^1 - \left(q_1^1 - q_3^1 - q_4^1 \right) \hat{\underline{s}}_3^1 . \tag{55}$$

Use of equations (31) and (48) leads at last to the linearized forms for angular position and rotation rate:

$$\begin{Bmatrix} \phi_1^j \\ \phi_2^j \\ \phi_3^j \end{Bmatrix} = \left[\Re_j \right] \begin{Bmatrix} q_2^1 + q_6^1 \\ q_5^1 \\ -\left(q_1^1 - q_3^1 - q_4^1 \right) \end{Bmatrix} \tag{56}$$

and

$$\begin{Bmatrix} \dot{\phi}_1^j \\ \dot{\phi}_2^j \\ \dot{\phi}_3^j \end{Bmatrix} = \left[\Re_j \right] \begin{Bmatrix} u_2^1 + u_6^1 \\ u_5^1 \\ -\left(u_1^1 - u_3^1 - u_4^1 \right) \end{Bmatrix} . \tag{57}$$

The *j*th umbilical portion of the GAF contribution due to the flotor for the *r*th generalized speed can now be expressed in terms of the coordinates and independent generalized speeds:

$$
{}^{j}Q_r^F = {}^{S_1}\underline{v}_r^{F_{U_j}} \cdot \underline{F}^{U_j} + {}^{S}\underline{\omega}_r^F \cdot \underline{M}^{U_j} = \begin{bmatrix} \sum_{r=1}^{6} v_{r1}^{U_j} \\ \sum_{r=1}^{6} v_{r2}^{U_j} \\ \sum_{r=1}^{6} v_{r3}^{U_j} \\ \sum_{r=1}^{6} \omega_{r1}^{U_j} \\ \sum_{r=1}^{6} \omega_{r2}^{U_j} \\ \sum_{r=1}^{6} \omega_{r3}^{U_j} \end{bmatrix}^T \begin{Bmatrix} F_1^{U_j} \\ F_2^{U_j} \\ F_3^{U_j} \\ M_1^{U_j} \\ M_2^{U_j} \\ M_3^{U_j} \end{Bmatrix}, \tag{58}
$$

where

$$
\begin{Bmatrix} F_1^{U_j} \\ F_2^{U_j} \\ F_3^{U_j} \\ M_1^{U_j} \\ M_2^{U_j} \\ M_3^{U_j} \end{Bmatrix} = \begin{bmatrix} k_{11}^{U_j} & \cdots & k_{16}^{U_j} \\ \vdots & \ddots & \vdots \\ k_{61}^{U_j} & \cdots & k_{66}^{U_j} \end{bmatrix} \begin{Bmatrix} x_1^{U_j} \\ x_2^{U_j} \\ x_3^{U_j} \\ \phi_1^{U_j} \\ \phi_2^{U_j} \\ \phi_3^{U_j} \end{Bmatrix} + \begin{bmatrix} c_{11}^{U_j} & \cdots & c_{16}^{U_j} \\ \vdots & \ddots & \vdots \\ c_{61}^{U_j} & \cdots & c_{66}^{U_j} \end{bmatrix} \begin{Bmatrix} \dot{x}_1^{U_j} \\ \dot{x}_2^{U_j} \\ \dot{x}_3^{U_j} \\ \dot{\phi}_1^{U_j} \\ \dot{\phi}_2^{U_j} \\ \dot{\phi}_3^{U_j} \end{Bmatrix} + \begin{Bmatrix} F_{b1}^{U_j} \\ F_{b2}^{U_j} \\ F_{b3}^{U_j} \\ M_{b1}^{U_j} \\ M_{b2}^{U_j} \\ M_{b3}^{U_j} \end{Bmatrix}, \tag{59}
$$

and the elongations, elongation rates, angles of twist, and twist rates are as defined in equations (43), (47), (56), and (57). The model is now ready for calibration and computer implementation.

6. IMPLEMENTATION IN AUTOLEV

A nonlinear, rigid-body model for the untethered ARIS; i.e., without umbilicals, with full actuator dynamics (masses and inertias), was previously developed using OnLine Dynamics' Autolev, a DOS-based interpreter specifically designed to solve dynamics problems using Kane's method.[11] The umbilical contributions developed above (eqs. (58) and (59)) were incorporated into that model by appropriately adding those contributions to the untethered-model GAFs. In Autolev, this required entering the locations of the umbilical attachment points, the orientations of the stator-fixed coordinate systems associated with the umbilicals, and the umbilical forces and moments determined above.

The geometric data required to include the umbilicals were determined from CAD models, such as in figure 3. Since umbilical stiffness and damping values were not available, representative estimates were entered and varied as needed for the process of model verification (described in section 7).

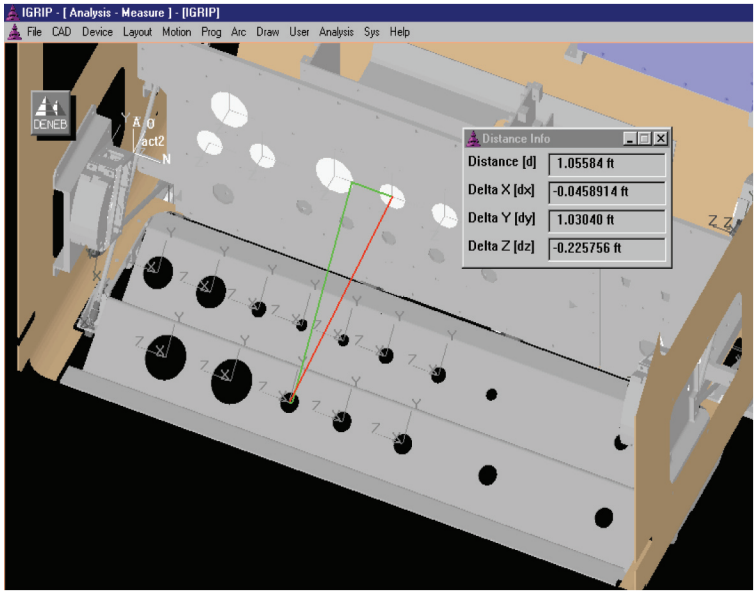

Figure 3. CAD-based technique for determining umbilical attachment locations.

After adding necessary terms to the Autolev model of ARIS, the code was compiled in the Autolev workspace. Autolev then auto-generated a C-program file containing the equations of motion and a numerical integration routine for their solution. Results of executing the C-program were plotted using Microsoft® Excel.

7. MODEL VERIFICATION

Numerous simulations were run to verify the model for special cases. The basic procedure was to reduce the actuator stiffness to very small levels and apply selected test forces (moments) through (about) the flotor center of mass. Corresponding simulations were compared between the full nonlinear model and appropriate (translational or torsional) single-degree-of-freedom truth models. Representative comparison checks are described in sections 7.1–7.8.

For each of the following comparisons, a single umbilical is assumed to be attached between the stator and the flotor center of mass. Umbilical biases are assumed to be zero. The umbilical coordinate system, $\hat{\underline{\xi}}_i$, is assumed to be aligned with the flotor-fixed coordinate system, $\hat{\underline{f}}_i$, when the flotor is in the reference position. Stiffness and damping terms that couple translation and rotation are all assumed to be zero. For forces (moments) applied through (about) the flotor mass center and for small-enough actuator stiffness, the ARIS system dynamics should approximate those of a simple second-order spring-mass-damper system (fig. 4).

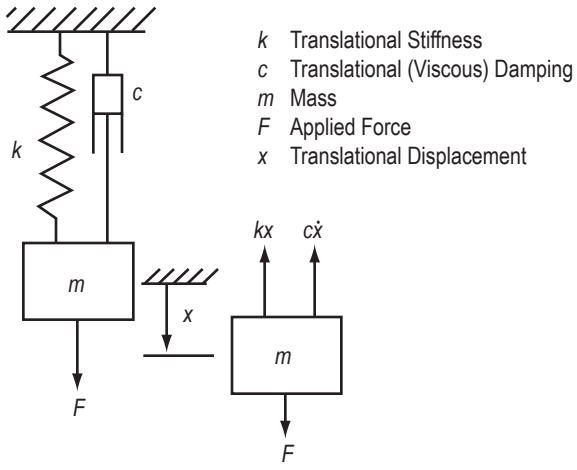

Figure 4. Translational single-degree-of-freedom truth model.

The flotor mass is assumed to be 55.6 slugs (1,790 lbm, 811.94 kg), and the central principal moments of inertia, 166.8 slug-ft^2 (5,371 lbm-ft^2, 226.34 kg-m^2). The umbilical stiffness matrix is assumed to be diagonal with each diagonal element set at 30 (lbf/ft for translational elements and lbf-ft/rad for rotational elements). The damping matrix is also assumed diagonal with all diagonal terms numerically equal but varied as needed to control the damping ratios, depending on the particular simulation.

7.1 Onboard Impulsive-Disturbance Force, No Damping

For the first test of the ARIS model, an impulsive disturbance force was applied directly to the flotor mass center along the $\underline{\hat{\xi}}_2$ direction, with zero damping. The disturbance was also applied to a simple spring-mass truth model with the same mass and stiffness. The impulse was approximated by a rapidly decaying exponential function:

$$\underline{F} = Ae^{-dt}\underline{\hat{\xi}}_2 \quad , \tag{60}$$

where d=100 s^{-1} and A=100 lbf (444.82 N). The two systems had identical sinusoidal responses (fig. 5) at the expected natural frequency of 0.7346 rad/s (0.1169 Hz).

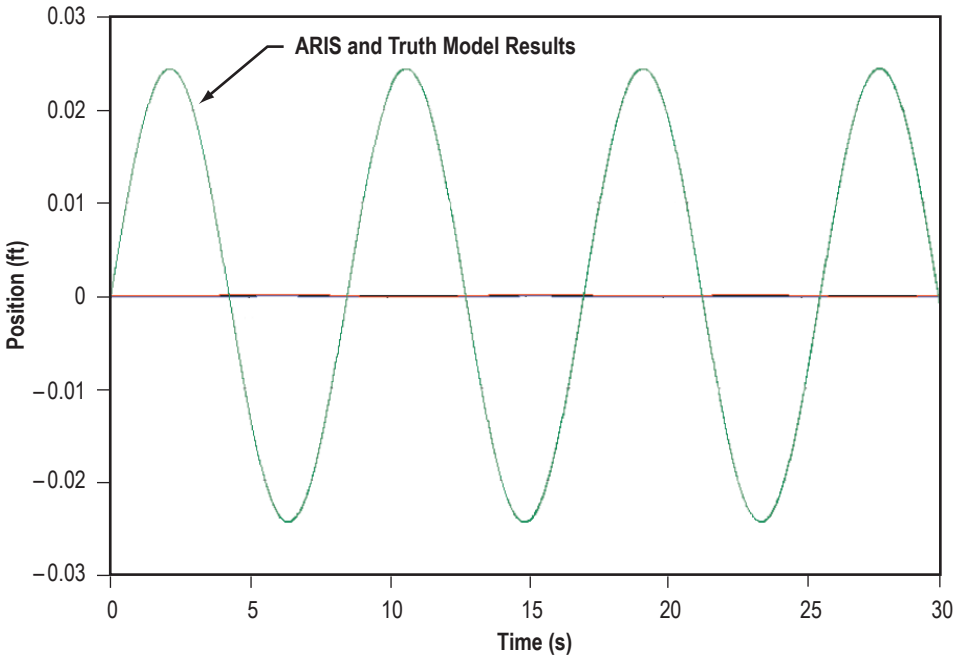

Figure 5. Translational displacement due to onboard impulsive-disturbance force.

7.2 Onboard Sinusoidal-Disturbance Force, With Damping

In a second test, a sinusoidal disturbance force with an amplitude of 3 lbf (13.34 N) and a frequency of ω was applied to the flotor mass center, again in the $\underline{\hat{\xi}}_2$ direction, using various frequency ratios, ω/ω_n, and damping factors, ζ. As before, the disturbance was also applied to a corresponding truth model. The two system responses were identical (figs. 6–8).

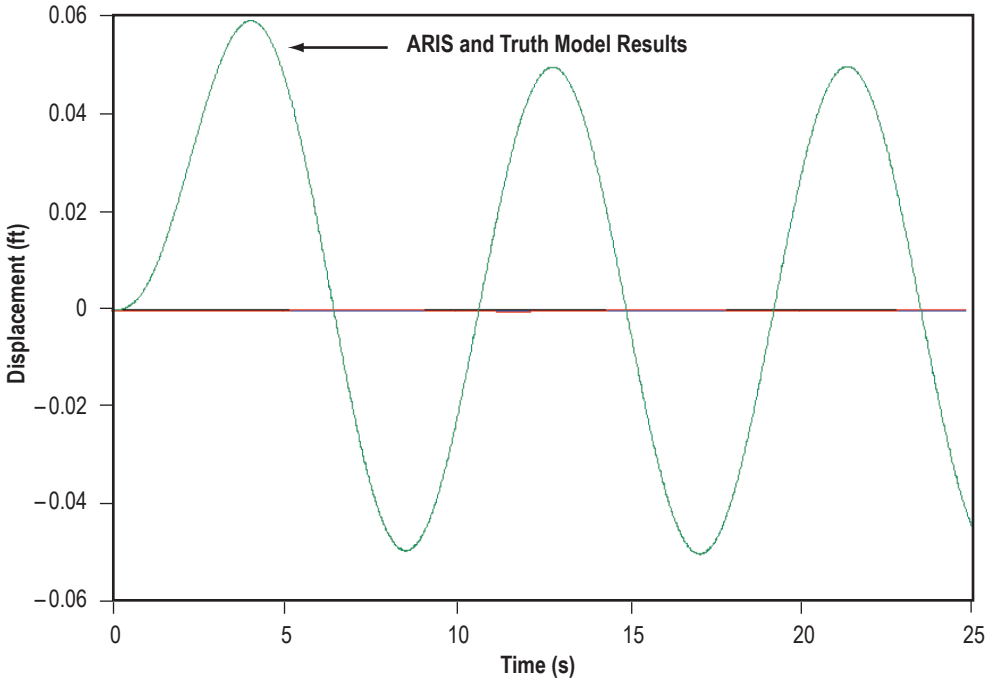

Figure 6. Translational displacement due to onboard sinusoidal-disturbance force with $\frac{\omega}{\omega_n} = 1$ and $\zeta = 1$.

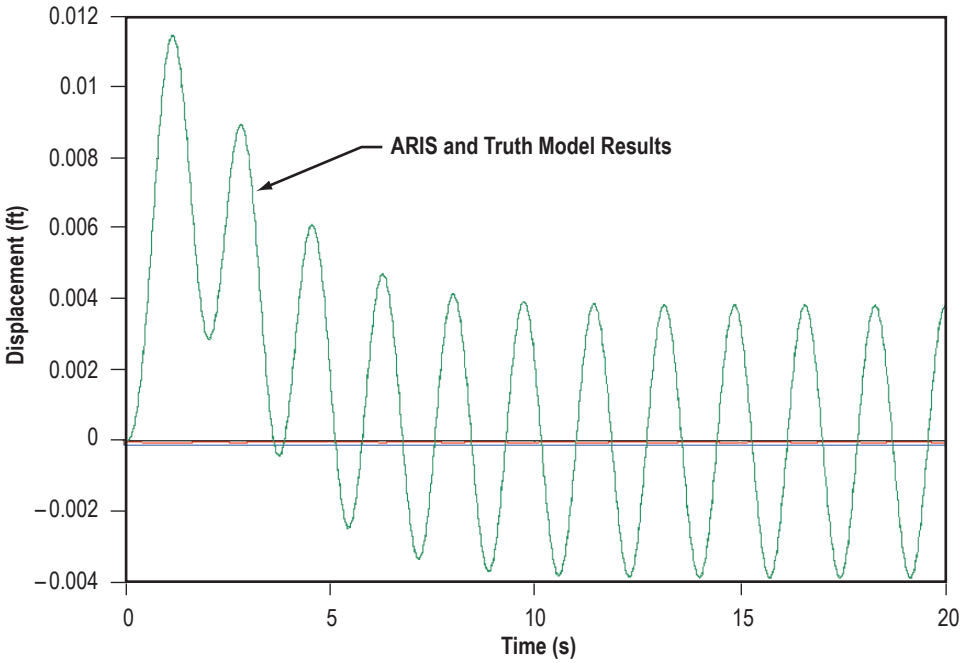

Figure 7. Translational displacement due to onboard sinusoidal-disturbance force with $\frac{\omega}{\omega_n} = 5$ and $\zeta = 1$.

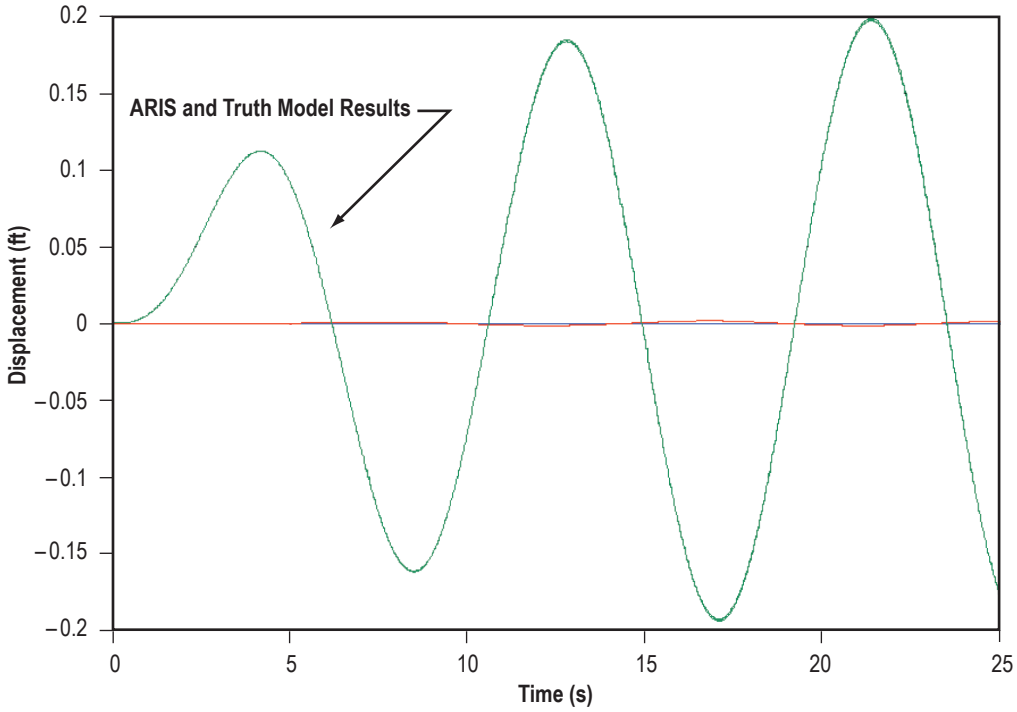

Figure 8. Translational displacement due to onboard sinusoidal-disturbance force with $\frac{\omega}{\omega_n} = 1$ and $\zeta = 0.25$.

7.3 Onboard Impulsive-Disturbance Moment, No Damping

To check the ARIS model rotational response, an impulsive disturbance moment was applied directly to the flotor at its mass center about the $\hat{\underline{\xi}}_2$ direction with zero damping. The disturbance was also applied to a simple rotational spring-mass truth model, with the same inertia and rotational stiffness. Again, the impulse was approximated by a rapidly decaying exponential function:

$$\underline{M} = Ae^{-dt}\hat{\underline{\xi}}_2 \ , \tag{61}$$

where d=100 s^{-1} and A=100 lbf-ft/s (135.58 N-m/s). The two systems had identical sinusoidal responses (fig. 9) at the expected natural frequency of 0.4241 rad/s (0.0675 Hz).

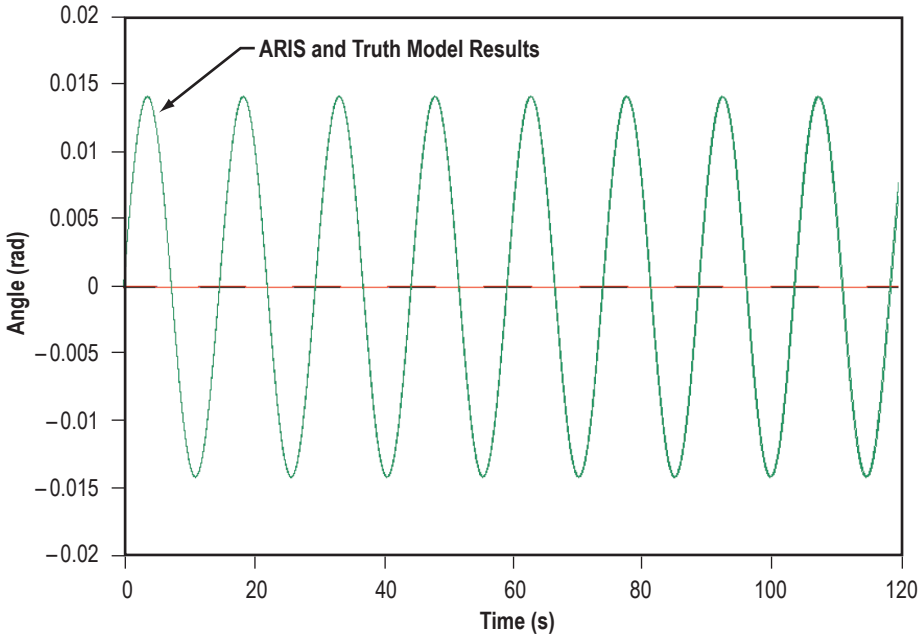

Figure 9. Rotational displacement due to onboard impulsive-disturbance moment.

7.4 Onboard Disturbance Moment, With Damping

To test the damped rotational response, a sinusoidal disturbance moment with amplitude 0.09 lbf-ft/s (0.122 N-m/s) and frequency, ω, was applied at the flotor mass center, about the $\hat{\underline{\xi}}_2$ direction, using various frequency ratios, ω/ω_n, and damping factors, ζ. The disturbance was also applied to a corresponding truth model. Again, the two system responses were identical (figs. 10–12).

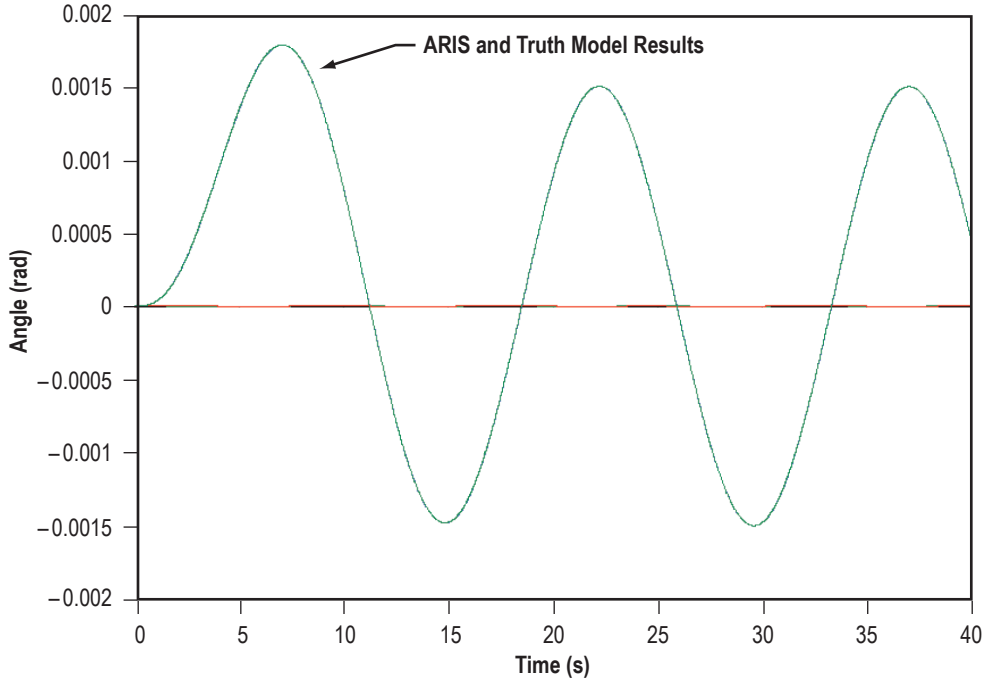

Figure 10. Rotational displacement due to onboard sinusoidal-disturbance moment with $\frac{\omega}{\omega_n} = 1$ and $\zeta = 1$.

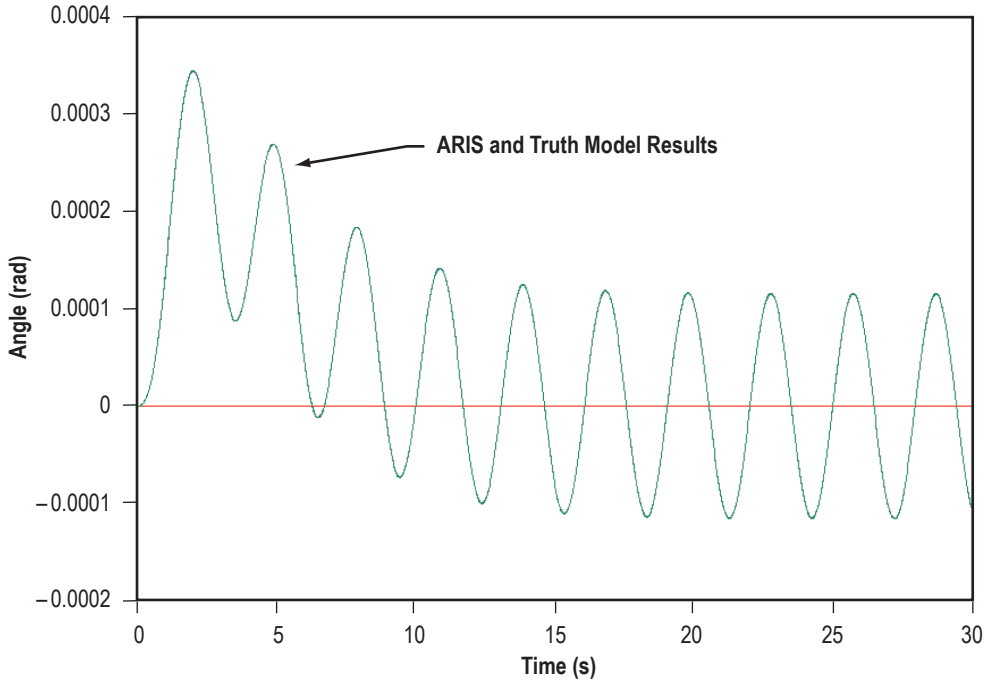

Figure 11. Rotational displacement due to onboard sinusoidal-disturbance moment with $\frac{\omega}{\omega_n} = 5$ and $\zeta = 1$.

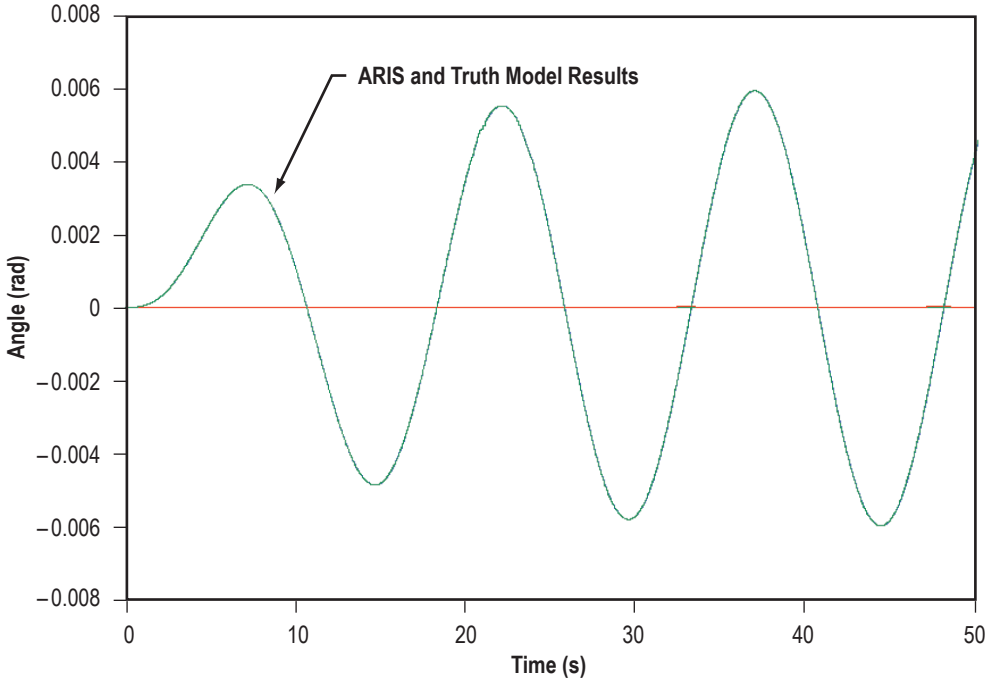

Figure 12. Rotational displacement due to onboard sinusoidal-disturbance moment with $\frac{\omega}{\omega_n} = 1$ and $\zeta = 0.25$.

7.5 Off-Board Translational Disturbance

In normal operation, the flotor will also be subject to off-board disturbances, which are transmitted via the ARIS umbilicals and actuators. With negligible actuator stiffness, the system response should match that of a corresponding truth model (fig. 13). A translational sinusoidal disturbance of amplitude 0.25 in (0.635 cm) was applied to the stator (base) in the $\hat{\underline{\xi}}_2$ direction with the ARIS umbilical oriented so that its stator attachment point was collinear with the flotor mass center, along the $\hat{\underline{\xi}}_2$ direction. (The flotor attachment point was assumed to be at the mass center, as before.) Various frequency ratios, ω/ω_n, and damping factors, ζ, were used with the flotor-to-stator relative displacements compared to those of the truth model. The responses of the two systems were identical (figs. 14–16).

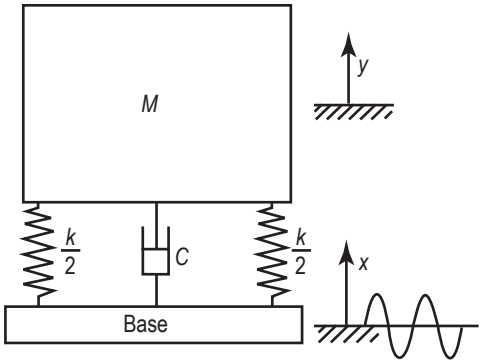

Figure 13. Translational single-degree-of-freedom truth model, with base motion.

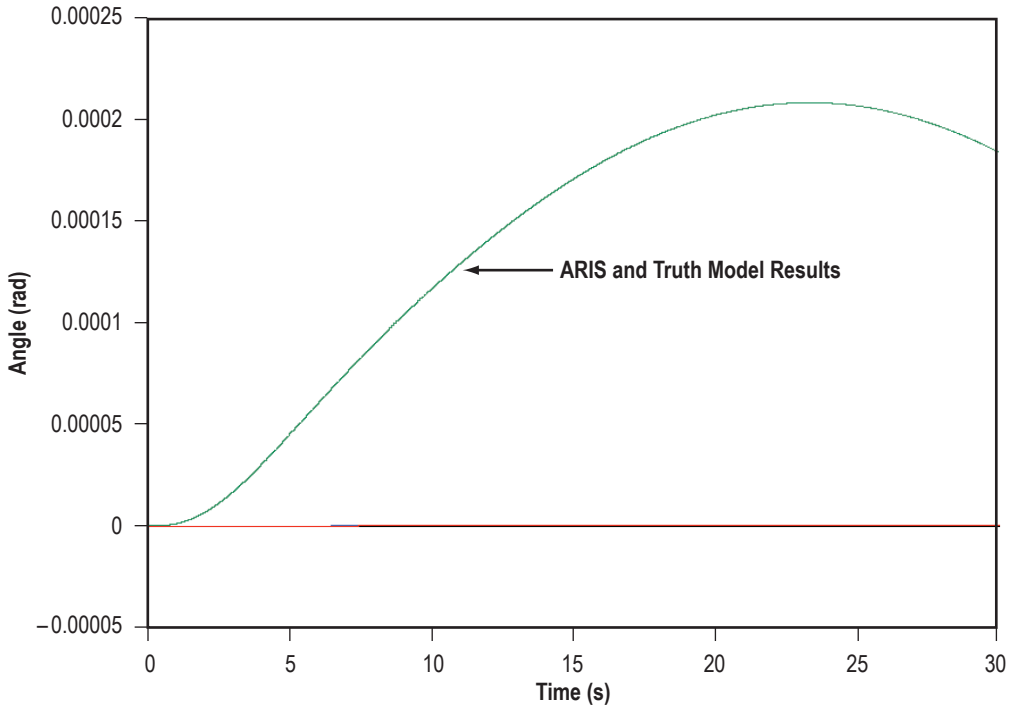

Figure 14. Translational displacement due to off-board sinusoidal position disturbance with $\frac{\omega}{\omega_n} = 0.1$ and $\zeta = 0.707$.

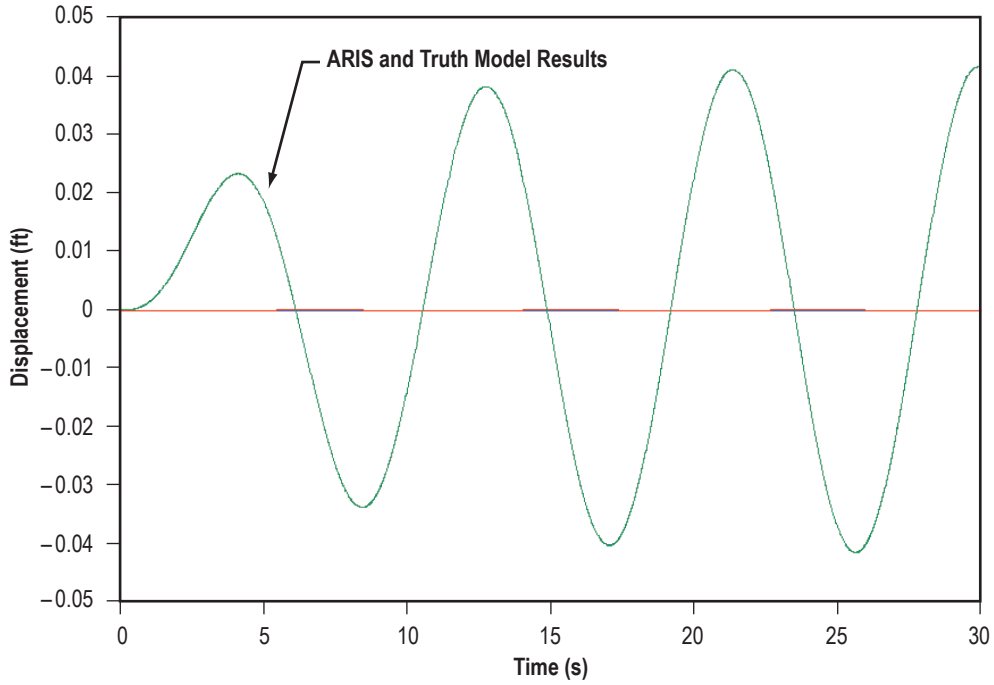

Figure 15. Translational displacement due to off-board sinusoidal position disturbance with $\frac{\omega}{\omega_n} = 1$ and $\zeta = 0.25$.

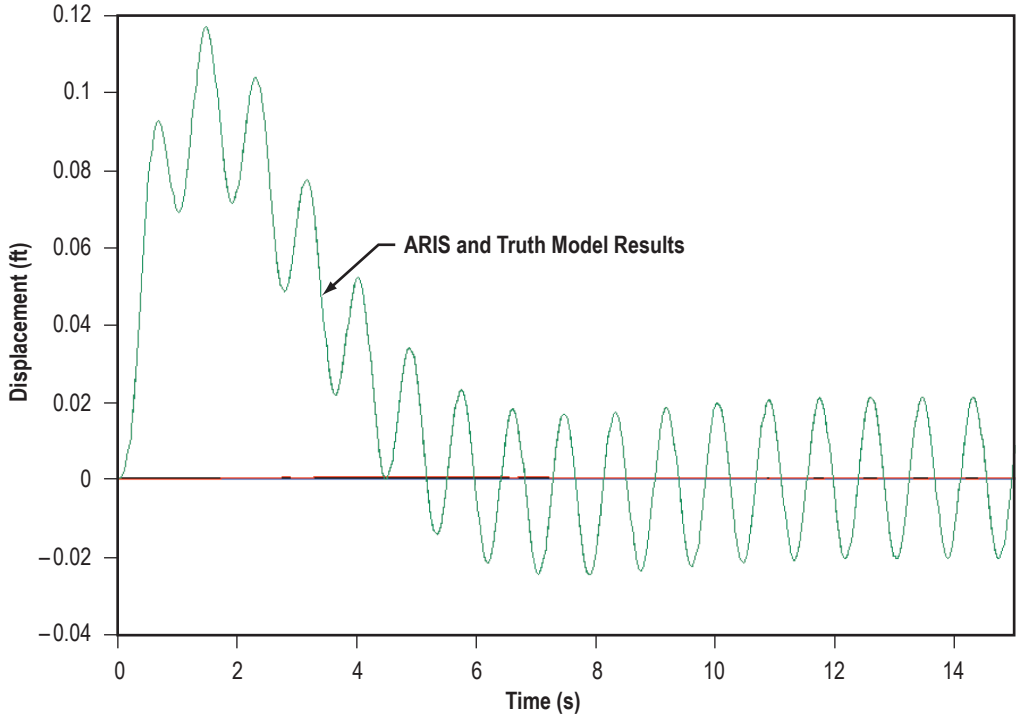

Figure 16. Translational displacement due to off-board sinusoidal position disturbance with $\frac{\omega}{\omega_n} = 10$ and $\zeta = 0.707$.

7.6 Off-Board Rotational Disturbance

A rotational sinusoidal disturbance, of amplitude 0.001 rad (0.0573°) was applied to the stator (base) about the $\hat{\underline{\xi}}_2$ direction with the ARIS umbilical attached and oriented as in the previous section. Various frequency ratios, ω/ω_n, and damping factors, ζ, were used with the flotor-to-stator relative rotations compared to those of the truth model. The responses of the two systems were identical (figs. 17–19).

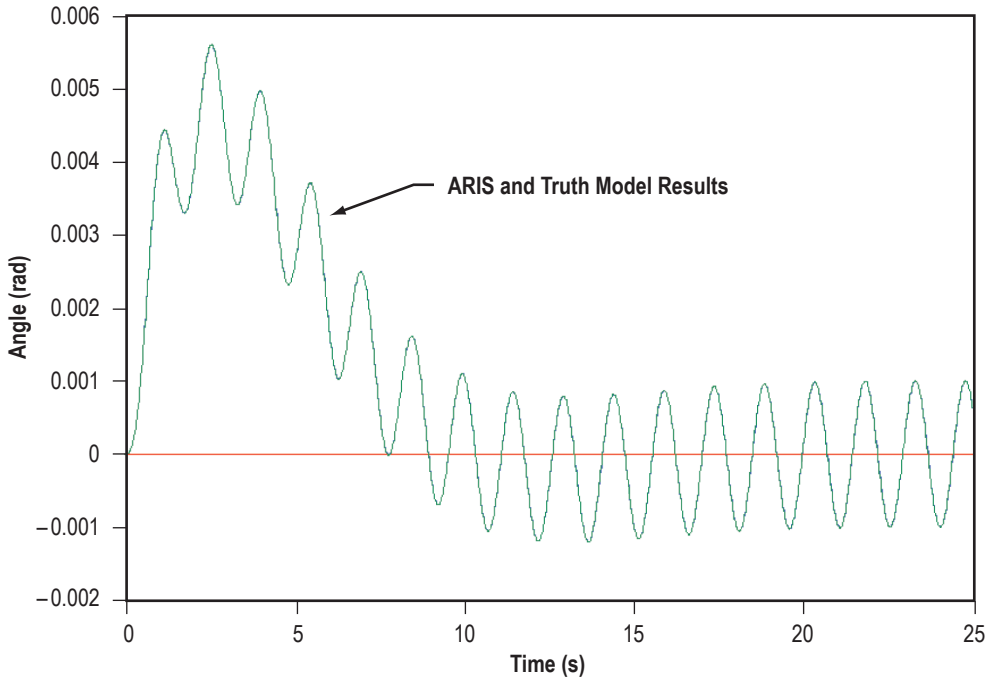

Figure 17. Rotational displacement due to off-board sinusoidal rotation disturbance with $\frac{\omega}{\omega_n} = 10$ and $\zeta = 0.707$.

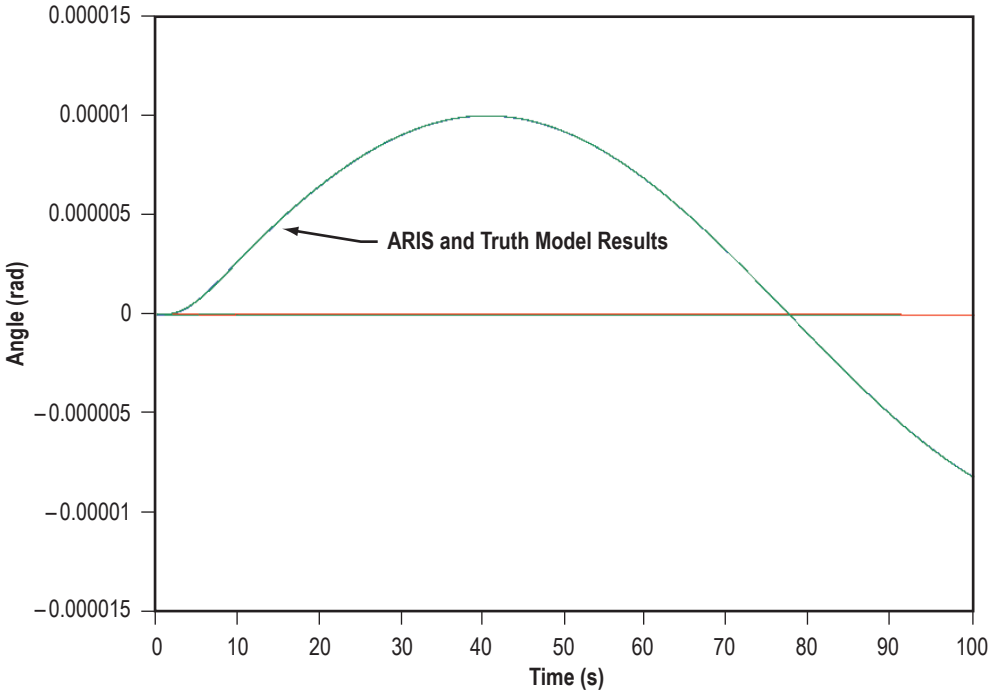

Figure 18. Rotational displacement due to off-board sinusoidal rotation disturbance with $\frac{\omega}{\omega_n} = 0.1$ and $\zeta = 0.707$.

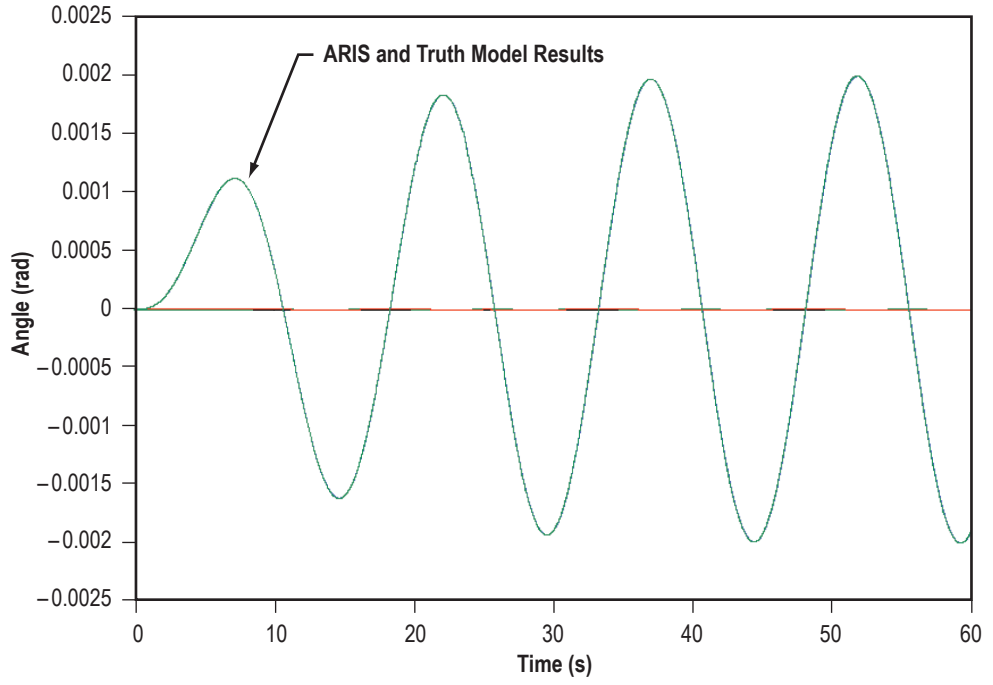

Figure 19. Rotational displacement due to off-board sinusoidal rotation disturbance with $\frac{\omega}{\omega_n} = 1$ and $\zeta = 0.25$.

7.7 Comparisons Using Nondiagonal Stiffness and Damping Matrices

Suppose now that the stiffness and damping matrices, $[K]$ and $[C]$, respectively, used for the above simulations are changed by selecting a new coordinate system, $\hat{\underline{\xi}}'_i$, rotated through $\left[\Re'\right]$ from the previous coordinate system, $\hat{\underline{\xi}}_i$:

$$\begin{Bmatrix} \hat{\underline{\xi}}'_1 \\ \hat{\underline{\xi}}'_2 \\ \hat{\underline{\xi}}'_3 \end{Bmatrix} = \left[\Re'\right] \begin{Bmatrix} \hat{\underline{\xi}}_1 \\ \hat{\underline{\xi}}_2 \\ \hat{\underline{\xi}}_3 \end{Bmatrix} = \left[\Re'\right]\left[\Re\right] \begin{Bmatrix} \underline{s}^1_1 \\ \underline{s}^1_2 \\ \underline{s}^1_3 \end{Bmatrix} . \tag{62}$$

Then the upper left and lower right block diagonal three-by-three submatrices, $\left[K_{11}\right]$ and $\left[K_{22}\right]$, of the (initially diagonal) stiffness matrix, $[K]$, become, respectively,

$$\left[K'_{11}\right] = \left[\Re'\right]\left[K_{11}\right]\left[\Re'\right]^T \tag{63}$$

and

$$\left[K'_{22}\right] = \left[\Re'\right]\left[K_{22}\right]\left[\Re'\right]^T . \tag{64}$$

Similar relationships hold for the damping matrix, $[C]$, and its corresponding submatrices. If the same disturbance force or moment is now applied as in any of the preceding simulations, then the resulting system motion should remain unmodified, which was shown to be the case.[12] This indicates that the ARIS model correctly handles cross-coupling among axes; i.e., full stiffness and damping submatrices, $\left[K_{11}\right]$, $\left[K_{22}\right]$, $\left[C_{11}\right]$, and $\left[C_{22}\right]$.

8. CONCLUSION

This TM has shown how multiple ARIS umbilicals, modeled as massless three-dimensional Hookean springs in parallel with three-dimensional viscous dampers, are to be included in the nonlinear Kane's model of ARIS. The umbilical force, moment, partial-velocity, and partial-angular-velocity terms were determined for the flotor contributions to the GAFs in Kane's dynamical equations.

Next, these modifications were incorporated into the ARIS Autolev simulation code. Simplifying assumptions were made to permit the comparison of the Autolev model's input responses to those of simple second-order truth models for selected test inputs. Numerous simulations, involving onboard and off-board force and moment disturbances, showed that the ARIS-model responses match those of the truth models. This indicates that the proposed model, when properly calibrated against experimental data, will provide a high-fidelity representation of ARIS for simulation and controller-design purposes.

REFERENCES

1. Bushnell, G.S.; Anderson, T.M.; Becraft, M.D.; and Jacot, A.D.: "Active Rack Isolation System Development for the *International Space Station*," *AIAA 1997–1203*, April 1997.

2. Bushnell, G.S.; and Becraft, M.D.: "Microgravity Performance Flight Characteristics of an *International Space Station* Active Rack Isolation Prototype System," *IEEE–0–7803–5276–9*, September 1999.

3. Hampton, R.D.; and Beech, G.S.: "A 'Kane's Dynamics' Model for the Active Rack Isolation System," *NASA/TM—2001–2110063*, 36 pp., Marshall Space Flight Center, AL, June 2001.

4. Kane, T.R.; and Levinson, D.A.: *Dynamics: Theory and Applications*, 379 pp., McGraw-Hill, Inc., New York, 1985.

5. Beech, G.S.; Hampton, R.D.; and Rupert, J.K.: "A 'Kane's Dynamics' Model for the Active Rack Isolation System: Part Two: Nonlinear Model Development Verification and Simplification," *NASA/TM—2004–213552*, 32 pp., Marshall Space Flight Center, AL, November 2004.

7. Beech, G.S.: *A High Fidelity Model for the Active Rack Isolation System*, Master's Thesis, 69 pp., The University of Alabama in Huntsville, Huntsville, AL, December 2000.

6. Thomson, W.T.: *Mechanical Vibrations*, 2nd Ed., Prentice-Hall, Inc., New York, 1953.

8. Rupert, J.K.; and Hampton, R.D.: "An Improved Umbilical Model for The Active Rack Isolation System," *AIAA 2000–0573*, January 2000.

9. Johnson, T.L.; and Tolson, H.R.: "Development of a Simulation Capability for the Space Station Active Rack Isolation System," *Specification NASA/CR—1998–206942*, Langley Research Center, March 1998.

10. Greenwood, D.T.: *Principles of Dynamics*, 2nd Ed., Prentice-Hall, Inc., New Jersey, 1988.

11. Kane, T.R.; and Levinson, D.A.: *Dynamics Online: Theory and Implementation with Autolev*™, 408 pp., Sunnyvale, CA, 1996.

12. Rupert, J.K.: *An Umbilical Model for the Active Rack Isolation System*, Masters Thesis, The University of Alabama in Huntsville, 2001.

REPORT DOCUMENTATION PAGE

Form Approved
OMB No. 0704-0188

1. AGENCY USE ONLY *(Leave Blank)*	2. REPORT DATE	3. REPORT TYPE AND DATES COVERED
	February 2005	Technical Memorandum

4. TITLE AND SUBTITLE

A "Kane's Dynamics" Model for the Active Rack Isolation System
Part Three: Addition of Umbilicals to the Nonlinear Model

5. FUNDING NUMBERS

6. AUTHORS

J.K. Rupert,* R.D. Hampton,** and G.S. Beech

7. PERFORMING ORGANIZATION NAME(S) AND ADDRESS(ES)

George C. Marshall Space Flight Center
Marshall Space Flight Center, AL 35812

8. PERFORMING ORGANIZATION REPORT NUMBER

M–1138

9. SPONSORING/MONITORING AGENCY NAME(S) AND ADDRESS(ES)

National Aeronautics and Space Administration
Washington, DC 20546–0001

10. SPONSORING/MONITORING AGENCY REPO NUMBER

NASA/TM—2005–213848

11. SUPPLEMENTARY NOTES

Prepared by the Engineering Systems Department, Engineering Directorate
*Dynetics, Inc., **United States Military Academy

12a. DISTRIBUTION/AVAILABILITY STATEMENT

Unclassified-Unlimited
Subject Category 88
Availability: NASA CASI 301–621–0390

12b. DISTRIBUTION CODE

13. ABSTRACT *(Maximum 200 words)*

In the late 1980s, microgravity researchers began to voice their concern that umbilical-transmitted energy could significantly degrade the acceleration environment of microgravity space science experiments onboard manned spacecraft. Since umbilicals are necessary for many experiments, control designers began to seek ways to compensate for these "indirect" disturbances.

Hampton, et al., used the Kane's method to develop a model of the active rack isolation system (ARIS) that includes (1) actuator control forces, (2) direct disturbance forces, and (3) indirect, actuator-transmitted disturbances. Their model does not, however, include the indirect, umbilical-transmitted disturbances. Since the umbilical stiffnesses are not negligible, these indirect disturbances must be included in the model. Until the umbilicals have been appropriately included, the model will be incomplete.

This Technical Memorandum presents a nonlinear model of ARIS with umbilicals included. Model verification was achieved by utilizing two commercial-off-the-shelf software tools. Various forces and moments were applied to the model to yield simulated responses of the system. Plots of the simulation results show how various critical points on an ARIS-outfitted international standard payload rack behave under the application of direct disturbances, indirect disturbances, and control forces. Simulations also show system response to a variety of initial conditions.

14. SUBJECT TERMS

ARIS, umbilicals, dynamics, control, math model

15. NUMBER OF PAGES

44

16. PRICE CODE

17. SECURITY CLASSIFICATION OF REPORT	18. SECURITY CLASSIFICATION OF THIS PAGE	19. SECURITY CLASSIFICATION OF ABSTRACT	20. LIMITATION OF ABSTRACT
Unclassified	Unclassified	Unclassified	Unlimited

National Aeronautics and
Space Administration
IS04
George C. Marshall Space Flight Center
Marshall Space Flight Center, Alabama
35812